A Study of MB-OFDM Wireless System over different UWB Channel Conditions

GBSR Naidu[1],D.Srinivasa rao[2],PMK Prasad[3]
[1,2,3]Faculty,Dept.of ECE,GMRIT,Rajam,A.P

Abstract –The demand for seamless mobile connectivity and wireless internet access across the globe has been increasing. OFDM has been shown to be very efficient in wireless and wire line communication over broadband channels. Frequency offset is mismatch between transmitter frequency and receiver frequency. Frequency offset is produced by unstable receiver clock generator or Doppler Effect. OFDM systems are very sensitive to these frequency offsets. The sensitivity is increased by increasing the number of sub carriers or constellation. Frequency offset degrades the performance of both channel estimation and symbol detection. Ultra-Wide Band (UWB) systems (e.g., impulse radios and transmitted reference schemes to name a few) offer improved ranging precision, better penetration through obstacles, higher data rate, and increased multipath or frequency diversity. By applying auto correlation or cross correlation techniques, the frequency offset of OFDM based UWB channels can be estimated.

Index Terms –OFDM, UWB, Frequency offset, BER

1. INTRODUCTION

The difference between the frequency of the oscillator in the transmitter and the receiver causes frequency offset which if not estimated and compensated could ruin the orthogonality of the sub-carriers thereby causing large bit errors in the received signal. Also the distortion of the signals while travelling through the channel and the movement of the mobility user causes synchronisation problems. Frequency offset (FO) arises from a number of factors: random Doppler frequency shifts, carrier frequency mismatch between transmitter and receiver oscillators and sampling frequency error between the ADCs. The FO causes severe reduction in signal amplitude and introduces intercarrier interferences (ICI) from the other subcarriers. As subcarriers are spaced out over the channel band- width, the FO must be minimized to a small fraction of the inter-subcarrier spacing in order to avoid severe bit error rate (BER) degradation from these detrimental effects. This thesis focuses on FO from carrier frequency mismatches and Doppler shifts only.The OFDM systems are very sensitive to the carrier frequency offset (CFO) and timing, therefore, before demodulating the OFDM signals at the receiver side, the receiver must be synchronized to the time frame and carrier frequency which has been transmitted.

1.1. Multi band OFDM

One of the most important advantages of OFDM over single-carrier schemes is its ability to cope with severe channel conditions, like narrowband interference or frequency-selective fading due to multipath, without complex equalization filters. Channel equalization is simplified because OFDM may be viewed as using many slowly-modulated narrowband signals rather than one rapidly-modulated wideband signal .In order to deal with low emitting power to avoid interference with other systems, an UWB implementation of OFDM [1] was proposed as Multi-Band OFDM (MBOFDM).

Multi band-OFDM transmission, five frequency groups are specified. All of these groups are divided into sub bands, each having a bandwidth greater than 528 MHz. In the each sub band, orthogonal frequency division multiplexing (OFDM) [2] is applied. Frequency hopping (FH) between different bands is supported so that the transmitted signal hops between Sub bands in every OFDM symbol duration is 312.5 ns. The sub-carrier allocation for MB-OFDM is shown in Fig 1.1. Each sub band contains 128 subcarriers. Ten of these are used as guard tones, twelve of the subcarriers are dedicated to the pilot signals, and 100 are for information. The remaining six tones are set to zero.Multiband OFDM was developed by the IEEE 802.15.3a and standardized by ECMA in. The physical layer and radio interface are well described.

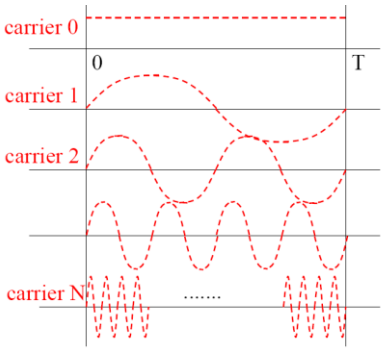

Fig 1.1: OFDM Sub-carrier allocation

Time-frequency spreading in Multiband OFDM facilitates multiple user access as each logical channel or piconet is defined by its unique TFC. The information is spread across three frequency bands to exploit frequency diversity and provide robustness against multipath and interference. The first band is commonly used by five out of seven TFCs to

facilitate the reception of beacon frames by user devices and hence aid their synchronization. For example, if the device uses a TFC of [1 2 3 1 2 3], the information in the first OFDM symbol is repeated on sub-bands 1 and 2, the information in the second OFDM symbol is repeated on sub-bands3 and 1, and that of the third OFDM symbol repeated in sub-bands 2 and 3.

1.2. Ultra Wide Band System

Ultra-Wideband (UWB) is a technology for transmitting information spread over a large bandwidth (>500 MHz) that should, in theory and under the right circumstances, be able to share spectrum with other users. Regulatory settings of FCC are intended to provide an efficient use of scarce radio bandwidth while enabling both high data rate "personal area network" (PAN) wireless connectivity and longer-range, low data rate applications as well as radar and imaging systems.

Ultra Wideband was traditionally accepted as pulse radio, but the FCC and ITU-R now define UWB in terms of a transmission from an antenna for which the emitted signal bandwidth exceeds the lesser of 500 MHz or 20% of the centre frequency. Thus, pulse-based systems—wherein each transmitted pulse instantaneously occupies the UWB bandwidth, or an aggregation of at least 500 MHz worth of narrow band carriers, for example in orthogonal frequency-division multiplexing (OFDM) fashion—can gain access to the UWB spectrum under the rules. Pulse repetition rates may be either low or very high. Pulse-based UWB radars and imaging systems tend to use low repetition rates, typically in the range of 1 to 100 mega pulses per second. On the other hand, communications systems favour high repetition rates, typically in the range of 1 to 2 giga-pulses per second, thus enabling short-range gigabit-per-second communications systems.

Each pulse in a pulse-based UWB system occupies the entire UWB bandwidth, thus reaping the benefits of relative immunity to multipath fading (but not to intersymbol interference), unlike carrier-based systems that are subject to both deep fades and intersymbol interference.

A significant difference between traditional radio transmissions and UWB radio transmissions is that traditional systems transmit information by varying the power level, frequency, and/or phase of a sinusoidal wave. UWB transmissions transmit information by generating radio energy at specific time instants and occupying large bandwidth thus enabling a pulse-position or time-modulation. The information can also be imparted (modulated) on UWB signals (pulses) by encoding the polarity of the pulse, the amplitude of the pulse, and/or by using orthogonal pulses. UWB pulses can be sent sporadically at relatively low pulse rates to support time/position modulation, but can also be sent at rates up to the inverse of the UWB pulse bandwidth. Pulse-UWB systems have been demonstrated at channel pulse rates in excess of 1.3 giga-pulses per second using a continuous stream of UWB pulses (Continuous Pulse UWB or "C-UWB"), supporting forward error correction encoded data rates in excess of 675 Mbit/s. Such a pulse-based UWB method using bursts of pulses is the basis of the IEEE 802.15.4a draft standard and working group, which has proposed UWB as an alternative PHY layer.

One of the valuable aspects of UWB radio technology is the ability for a UWB radio system to determine "time of flight" of the direct path of the radio transmission between the transmitter and receiver at various frequencies. This helps to overcome multi path propagation, as at least some of the frequencies pass on radio line of sight. With a cooperative symmetric two-way metering technique distances can be measured to high resolution as well as to high accuracy by compensating for local clock drifts and stochastic inaccuracies.

Another valuable aspect of pulse-based UWB [3] is that the pulses are very short in space (less than 60 cm for a 500 MHz wide pulse, less than 23 cm for a 1.3 GHz bandwidth pulse), so most signal reflections do not overlap the original pulse, and thus the traditional multipath fading of narrow band signals does not exist. However, there still is multipath propagation and inter-pulse interference for fast pulse systems which have to be mitigated by coding techniques.

2. MULTI BAND OFDM BASED UWB SYSTEM MODEL

2.1. Multi band OFDM PHY Layer

A multi-band OFDM system [4] divides the available bandwidth into smaller non-overlapping sub bands such that the bandwidth of a single sub-band is still greater than 500MHz (FCC requirement for a UWB system). The system is denoted as an ‘UWB-OFDM’ system because OFDM operates over a very wide bandwidth, much larger than the bandwidth of conventional OFDM systems. OFDM symbols are transmitted using one of the sub-bands in a particular time-slot. The sub-band selection at each time-slot is determined by a Time-Frequency Code (TFC). The TFC is used not only to provide frequency diversity in the system but also to distinguish between multiple users. The proposed UWB system utilizes five sub-band groups formed with 3 frequency bands (called a band group) and TFC to interleave and spread coded data [5] over 3 frequency bands. Four such band groups with 3 bands each and one band group with 2 bands are defined within the UWB spectrum mask.

There are also four 3-band TFCs and two 2-band TFCs, which, when combined with the appropriate band groups provide the capability to define eighteen separate logical channels or independent piconets. Devices operating in band group #1 (the three lowest frequency bands) are selected for the mandatory mode (mode #1) to limit RF phase noise degradations under low-cost implementations.

Fig. 2.1 shows the presence of a time frequency kernel in a typical OFDM TX architecture. Time-frequency kernel produces carriers with frequencies of 3.432MHz, 3.960MHz and 4.488MHz, corresponding to center frequency of sub band 1, 2 and 3. The MB-OFDM [6] based UWB PHY layer proposal submitted to IEEE 802.15.3a working sub-committee for WPANs specifies parameters for different modules of PHY layer.

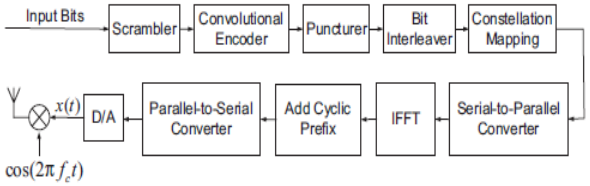

Fig 2.1: TX Architecture of an MB-OFDM System

From the total available bandwidth of 7.5GHz (3.1-10.6 GHz), usage of 1.5GHz (3.1-4.75 GHz) is set mandatory for all MB-OFDM devices. Although sub-band bandwidth is required to be greater than 500 MHz (FCC requirement as stated earlier), hardware constraints impose using as narrow bandwidth as possible. Hence, a sub-band of 528 MHz was proposed in, because it can be generated using simpler synthesizer circuits.

2.2. UWB Propagation Channel Model

In order to evaluate different PHY layer proposals, IEEE 802.15.3a channel modeling sub-committee proposed a channel model for realistic UWB environments. During 2002 and 2003, the IEEE 802.15.3 Working Group for Wireless Personal Area Networks and especially its channel modeling subcommittee decided to use the so called modified Sale–Valenzuela model (SV) as a reference UWB channel model [7]. The real valued model is based on the empirical measurements originally carried out in indoor environments in 1987. Due to the clustering phenomena observed at the measured UWB [9] indoor channel data, the model proposed by IEEE 802.15 is derived from Saleh and Valenzuela using a lognormal distribution rather than an original Rayleigh distribution for the multi-path gain magnitude. An independent fading mechanism is assumed for each cluster as for each ray within the cluster. In the SV models, both the cluster and ray arrival times are modeled independently by Poisson processes. The multi-path channel [10] impulse response can be expressed as

$$h(t) = \lambda \sum_{l \geq 0} \sum_{k \geq 0} \alpha_{k,l}\, \delta(t - T_1 - \tau_{k,l}) \quad (1)$$

Where k ,l, α is the real-valued multi-path gain for cluster l and ray k. The lth cluster arrives at time l T and its k th ray arrives at k, l, τ which is relative to the first path in cluster l,

i.e. 0 0, = l τ. The amplitude k, l, α has a log-normal distribution and the phase k, l,α is chosen from {0, π} with equal probability.

The baseband equivalent of the channel impulse response inqthband is given by,

$$h^q(i) = x \sum_{l=0}^{L} \sum_{k=0}^{K} \alpha_{k,l} e^{-j2\Pi f_q (T_1 + \tau K_{k,l})} p(iT_s - T_l - \tau_{k,l} - \tau_0); 0 \leq i \leq C-1 \quad (2)$$

where, $p(iT_s - T_l - \tau_{k,l} - \tau_0)$ is the delayed impulse response of the combined transmit and receive filter; $T_s$is the sampling time; $T_l$denotes the delay of the lth cluster, k ,l denotes the arrival time of kth ray in the lth cluster; o is the delay introduced to satisfy causality; $q_f$is the centre frequency of qth band; k ,l is the lognormal distributed multipath gain coefficient ; is the lognormal shadowing and C is the length of the impulse response. The channel coefficients are defined as

$$\alpha_{k,l} = p_{k,l} \beta_{k,l}$$

3. FREQUENCY-OFFSET ESTIMATION TECHNIQUE

CFO [3] can produce Inter Carrier Interference (ICI) which can be much worse than the effect of noise on OFDM systems. Therefore, it is important for it to be estimated and compensated for. Many algorithms have been proposed for estimating the carrier frequency offset. CFO estimation can be done in two ways either time domain based approach or frequency domain based approach. It is shown that the frequency domain based approach which is our proposed method offers better CFO estimation than the time domain [11] based approaches.

3.1. CFO Performance Analysis

For time-variant UWB channels, we first split the preamble in each band into two5 parts (left and right) by a simple abrupt channel change detection algorithm. We denote these parts by *p*-th preamble part with *p* = 1 and 2 for the left and right part, respectively. The underlying idea is that correlation-based estimators require identical channel output preamble symbols, and due to the abrupt change, the channel outputs corresponding to these two parts will not be identical, and hence should not be cross correlated. Next we estimate CFO based on each part, and then appropriately average the CFO estimates.

For time-invariant UWB channels, since they are the special cases of time-variant channels with the steady-state probability vector [1, 0] *T* . We can apply the method developed for the time-variant channel except with the following changes: we skip the abrupt channel change detection step, set the left part of the preamble in each band to be the preamble itself and hence null the right part. There are lot of correlation based estimators for frequency offset estimation, but blue based estimator is used for the estimation.

3.2. Proposed Methods

3.2.1 Method A (for the estimation of carrier frequency offset)

$$\theta q(m) = \upsilon q + \frac{N}{2\pi d(m)} \tan^{-1}(B(m)) \quad (3)$$

Where

$$B(m) = \frac{\Im\{Gq(m)\} + \Im\{Nq(m)\}}{Qq(m)Eq + \Re\{Gq(m)\} + \Re\{Nq(m)\}} \quad (4)$$

Where

$\Re\{.\}, \Im\{.\}$ are the real and the imaginary parts of {.}, respectively, and $\tan^{-1}$ is the four-quadrant arctangent function. For high SNR, we can approximate

$$\theta q(m) \approx \upsilon q + \frac{N}{2\pi d(m)} \frac{\Im\{Gq(m)\} + \Im\{Nq(m)\}}{Qq(m)Eq} \quad (5)$$

Preamble Patterns 1 & *2:* The preamble structure in each band is the same and adjacent identical parts have the same distance of 3*M*0. So $d(m) = 3mM0$ and $Q_q(m) = (Lq - m)$.

After straight-forward calculation, the *m*-th row, *n*-th column element of $C_{\theta q,p}$ can be expressed as

$$C_{\theta q-p}(m,n) = \frac{N^2\sigma^2}{4\pi^2 (3M_0)^2 Eq-p)(L_{q-p} - m)(L_{q-p} - n)}$$

$$\begin{cases} m + \dfrac{(L_{q-p} - m)N\sigma^2}{2E_{q-p}}, & if\ m = n \,\&\, m < L_{q-p}/2 \\ (L_{q-p} - m) + \dfrac{(L_{q-p} - m)N\sigma^2}{2E_{q-p}}, & if\ m = n \,\&\, m \geq L_{q-p}/2 \\ \min(m,n) & if\ m \neq n \,\&\, m + n < L_{q-p} \\ L_{q-p} - \max(m,n) & if\ m \neq n \,\&\, m + n \geq L_{q-p} \end{cases} \quad (6)$$

Preamble Patterns 3 & *4:* All possible correlation distances for the patterns 3 and 4 in all three bands are *{M*0, 5*M*0, 6*M*0, 7*M*0, 11*M*0, 12*M*0, 13*M*0, 17*M*0, 18*M*0,19*M*0*}*, which can be grouped into 3 categories: *{d*1(*m*) = 6*mM*0, $1 \leq m \leq Hq,p,1$*}*, *{d*2(*m*) = (6(*m*−1)+1)*M*0, $1 \leq m \leq Hq,p,2$*}*, and *{d*3(*m*) = (6*m*−1)*M*0, $1 \leq m \leq Hq,p,3$*}*, where *Hq,p*,1, *Hq,p*,2, and *Hq,p*,3 are design parameters. Let *Dq,p* denote the total number of periods (including null symbol Intervals) of the preamble used to calculate the correlation with the correlation distance d_i the *p*-th part in the *q*th band, counting from the first non-zero preamble period to the last non-zero preamble period used in the correlation term. *Dq,p*,1 is a special case, which is separated into $D_{q,p,1}$ and $D^e_{q,p,1}$, corresponding to the correlation distance 6*mM*0 on the odd symbol indices and the even symbol indices, respectively. Then $N^o_{q,p,1} = D^o_{q,p,1} M_0$

and $Nq, p, i = Dq, p, iMo \ \ for\ i = 1,2,3$

For the correlation term with a correlation distance $d_i(m)$ becomes

$$\theta_{q-p,i}(m) \approx \upsilon q + \frac{N}{2\pi di(m)} \frac{\Im\{G_{q-p,i}(m)\} + \Im\{N_{q-p,i}(m)\}}{Q_{q-p,i}(m)\ E_{q-p}} \quad (7)$$

Where

$$Q_{q-p,i}(m) = Q^o_{q-p,1}(m) + Q^e_{q-p,1}(m)$$

$$Q^o_{q-p,1}(m) = \left[\frac{N^o_{q-p,1} - d_1(m) - M_o}{6M_o} \right] + 1$$

$$Q^e_{q-p,1}(m) = \left[\frac{N^e_{q-p,1} - d_1(m) - M_o}{6M_o} \right] + 1$$

$$Q_{q-p,1}(m) = \left[\frac{N_{q-p,1} - d_i(m) - M_o}{6M_o} \right] + 1 \ for\ i = 2,3 \quad (8)$$

The covariance matrix can be expressed as

$$C_{\theta\ q-p} = \begin{bmatrix} C^{(1,1)}_{\theta}, C^{(1,2)}_{\theta}, C^{(1,3)}_{\theta} \\ C^{(2,1)}_{\theta}, C^{(2,2)}_{\theta}, C^{(2,3)}_{\theta} \\ C^{(3,1)}_{\theta}, C^{(3,2)}_{\theta}, C^{(3,3)}_{\theta} \end{bmatrix}_{q-p} \quad (9)$$

The final equation for the *m*-th row, *n*-th column element of $C\theta_{q-p}$ can be expressed as

$$C^{(2,3)}_{\theta_q}(m,n) = \frac{N^2\sigma^2}{4\pi^2 E_q} \frac{1}{d_2(m)d_3(n)\, Q_{q,2}(m)Q_{q,3}(n)}$$

$$-\frac{1}{2}\left(\left\langle \frac{N_{q,3} - M_o}{6M_o} \right\rangle + \left\langle \frac{N_{q,2} - M_o}{6M_o} \right\rangle \right) + m + n - 2,$$

$$if\ d_2(m) + d_3(n) < \min(N_{q,2}, N_{q,3})$$

$$-\frac{1}{2}\left(\left\langle \frac{\max(N_{q,2}, Nq,3) - M_o}{6M_o} \right\rangle - m - n + 2 \right)$$

$$if\ \min(N_{q,2}, N_{q,3}) \le d_2(m) + d_3(n) < \max(N_{q,2}, N_{q,3}) \tag{10}$$

3.2.2 Method B (for the estimation of carrier frequency offset)

Method B is another proposed method for the comparison of estimation performance .uses another high SNR approximation is

$$\theta_{q,p}(m) \approx \upsilon_q + \frac{N}{2\pi d(m)} \frac{\Im\{G_{q,p}(m)\}}{Q_{q,p}(m)E_{q,p}} \tag{11}$$

After straight forward calculations the covariance matrix for the different preamble patterns can be expressed as

For preamble patterns 1&2: The covariance matrix for the preambles. Here m rows and n columns

$$C_{\theta q}(m,n) = \frac{N^2\sigma^2}{4\pi^2(3M_0)^2\ E_q} \frac{1}{mn(L_q-m)(L_q-n)} \times \begin{cases} \min(m,n), & if\ m+n < L_q \\ L_q - \max(m,n), & if\ m+n \ge L_q \end{cases} \tag{12}$$

For preamble patterns 3&4: The covariance matrix for the preambles 3&4.m rows and n columns

$$C_{\theta q}^{(i,1)}(m,n)\Big| i = 2,3 = \frac{N^2\sigma^2}{4\pi^2 E_q} \frac{1}{d_i(m)d_i(n)\max(Q_{q,i}(m), Q_{q,i}(n))} \tag{13}$$

3.2.3 The hybrid CRB (HCRB) for OFO estimator in the UWB MB-OFDM system

The corresponding low-pass-equivalent time-domain received samples

$$r_q\left(t_l^q(i)\right) = e^{j\varphi} e^{j2\pi\upsilon q_l^{tq(i)/N}} x_q\left(t_l^q(i)\right) + n\left(t_l^q(i)\right) \tag{14}$$

Where $\{n(t_l^q(i))\}$, represents independent and identically-distributed, circularly-symmetric complex Gaussian noise samples with zero mean and variance

$$\sigma^2 = E\left\{\left|n(t_l^q(i))\right|^2\right\}$$

The above signal can be expressed in matrix form

$$r = e^{j\varphi} W(\upsilon)\ Sh + n$$

$$\begin{aligned} Where \quad r &= \left[r_1^T \quad r_2^T \quad r_3^T\right]^T, \\ r_q &= \left[r_q(0), r_q(1), \ldots, r_q(N-1)\right]^T \\ h &= \left[h_1^T \quad h_2^T \quad h_3^T\right]^T, \\ h_q &= \left[h_q(0), h_q(1), \ldots, h_q(K')\right]^T \\ W(\upsilon) &= diag\ \{W_1(\upsilon), W_2(\upsilon), W_3(\upsilon)\} \\ W_q(\upsilon) &= diag 1.e^{i2\pi bq\upsilon/N}, e^{j2\pi 2bq\upsilon/N}, \ldots, \\ & \quad e^{j2\pi(N-1)bq\upsilon/N}\ \} \\ & n = \left[n(0), n(1), \ldots, n(3N-1)\right]^T \\ & S = diag\ \{S_1, S_2, S_3\} \end{aligned} \tag{15}$$

and ***Sq*** is an $N \times K$ matrix with the (n, k) the element given by $(n_0 + n - k)$. $n_0\Delta = T_0/Ts$ and $K\_$ is the maximum number of sample-spaced channel taps.

$$\begin{aligned} \left[J_D\right]_{i,j} &= E_h\left[tr\left[C_r^{-1}\frac{\partial C_r}{\partial \alpha_i} C_r^{-1}\frac{\partial C_r}{\partial \alpha_j}\right]\right. \\ &\quad \left. + 2\Re\left[\frac{\partial m_r^H}{\partial \alpha_i} C_r^{-1}\frac{\partial m_r}{\partial \alpha_j}\right]\right] \\ J_p &= \begin{bmatrix} 0_{2\times 2} & 0_{2\times 3K'} \\ 0_{3K'\times 2} & Z \end{bmatrix} \\ Z &= -E\left[\frac{\partial^2\ In\ ph(h)}{\partial h^2}\right] \end{aligned} \tag{16}$$

After straight forward calculation we, obtain

$$\begin{aligned} \left[J_D\right]_{1,1} &= \frac{8\pi^2}{N^2\sigma_n^2} tr\left[S^H \wedge^2 SR_h\right] \\ \left[J_D\right]_{1,2} &= \left[J_D\right]_{2,1} = \frac{4\pi}{N\sigma_n^2} tr\left[S^H \wedge SR_h\right] \\ \left[J_D\right]_{2,2} &= \frac{2}{\sigma_n^2} tr\left[S^H \wedge SR_h\right] \\ \left[J_D\right]_{1,k\ge 3} &= \left[J_D\right]_{k\ge 3,1} = \left[J_D\right]_{2k\ge 3,} = \left[J_D\right]_{k\ge 3,2} = 0 \end{aligned} \tag{17}$$

Then, the HCRB for the OFO estimation in the MB-OFDM system is given by

$$HCRB = \left[J_B^{-1}\right]_{1,1} = \left[J_D\right]_{1,1} - \left[J_D\right]_{2,2}^{-1}\left[J_D\right]_{2,1}\Big)^{-1} \tag{18}$$

4. RESULTS AND DISCUSSIONS

Figs. 4.1 and 4.2 present the MSEs of the proposed methods (Method A and Method B) for the preamble patterns 1 (or equivalently 2) and 3 (or equivalently 4), respectively, for a Time-invariant channel. Method A gives the minimum MSE, which is quite close to the hybrid Cramer-Rao bound (HCRB) at moderate and high SNRs. All proposed methods perform better than the first set of reference methods, and the improvements of the proposed methods are more significant for the preamble patterns 3 and 4.

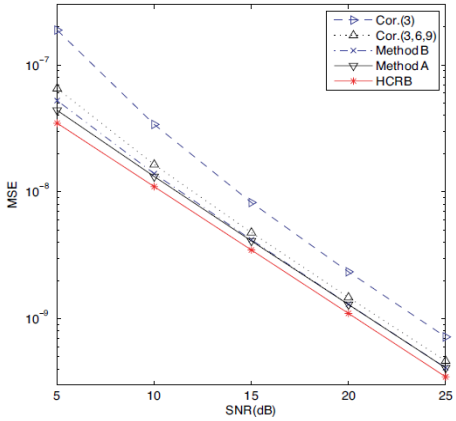

Figure 4.1: The normalized OFO estimation performance comparison in a time invariant channel for the preamble pattern 1 (or equivalently 2).

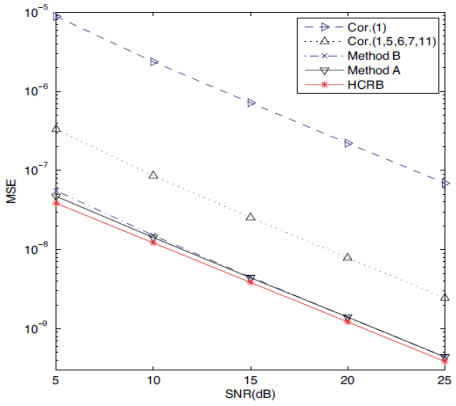

Figure 4.2: The normalized OFO estimation performance comparison between the proposed method and the first set of reference methods in a time-invariant Channel for the preamble pattern 3 (or equivalently 4).

5. CONCLUSION

The frequency offset estimation method presented in this project for MB-OFDM based UWB Systems is based on pilot tones. Oscillator frequency mismatch introduces different carrier-frequency offsets in different bands of MB-OFDM systems. The proposed estimators are adaptive such that when a sudden channel change is detected during the preamble duration the estimator designed for such a time-variant scenario is used, otherwise the estimator developed for the time-invariant channel is applied. For systems with no sudden channel changes, the latter estimator can be solely implemented for implementation simplicity. Our proposed approach can be applied to other multi-band systems or similar frequency hopped Systems.

REFERENCES

[1] M. Z. Win and R. A. Scholtz, "Impulse radio: how it works," IEEE Commun. Lett., vol. 2, no. 2, pp. 36-38, Feb. 1998.
[2] M. Z. Win and R. A. Scholtz, "Ultra-wide bandwidth time-hopping spread-spectrum impulse radio for wireless multiple-access communications," IEEE Trans. Commun., vol. 48, no. 4, pp. 679-691, Apr. 2000.
[3] T. Q. S. Quek and M. Z. Win, "Analysis of UWB transmitted reference communication systems in dense multipath channels," IEEE J. Select. Areas Commun., vol. 23, no. 9, pp. 1863-1874, Sept. 2005.
[4] A. Giorgetti, M. Chiani, and M. Z. Win, "The effect of narrowband interference on wideband wireless communication systems," IEEE Trans. Commun., vol. 53, no. 12, pp. 2139-2149, Dec. 2005.
[5] M. Z. Win, "A unified spectral analysis of generalized time-hopping spread-spectrum signals in the presence of timing jitter," IEEE J. Select. Areas Commun., vol. 20, no. 9, pp. 1664-1676, Dec. 2002.
[6] A. Ridolfi and M. Z. Win, "Ultrawide bandwidth signals as shot-noise: a unifying approach," IEEE J. Select. Areas Commun., vol. 24, no. 4, pp. 899-905, Apr. 2006.
[7] A. Batra, et. al., "Multi-band OFDM physical layer proposal for IEEE 802.15 task group 3a," IEEE P802.15-03/268r3, Orlando, FL, USA, Mar. 2004.
[8] IEEE 802.15 working group for wireless personal area networks (WPANs)' "Multi-band OFDM physical layer proposal for IEEE 802.15 task group 3a," Mar. 2004.
[9] Standard ECMA-368,"High rate ultra wideband PHY and MAC standard," Dec. 2005.
[10] L. J. Cimini, "Analysis and simulation of a digital mobile channel using orthogonal frequency division multiplexing," IEEE Trans. Commun., vol. 33, pp. 665-675, July 1985.
[11] J. A. C. Bingham, "Multicarrier modulation: an idea whose time has come," IEEE Commun. Mag., vol. 28, no. 5, pp. 5-14, May 1990.
[12] D. Dardari and V. Tralli, "High-speed indoor wireless communications at 60 GHz with coded OFDM," IEEE Trans. Commun., vol. 47, no. 11, pp. 1709-1721, Nov. 1999.
[13] D. Dardari, M. G. Martini, M. Mazzotti, and M. Chiani, "Layered video transmission on adaptive OFDM wireless systems," Eurasip J. Applied Signal Processing, Hindawi ublishing Corp., vol. 10, pp. 1557-1567, 2004.
[14] D. Dardari, "Ordered subcarrier selection algorithm for OFDM based high-speed WLANs," IEEE Trans. Wireless Commun., vol. 3, no. 5, pp. 1452-1458, Sept. 2004.
[15] D. Dardali, V. Tralli, and A. Vaccari, "A theoretical characterization of nonlinear distortion effects in OFDM systems," IEEE Trans. Commun., vol. 48, no. 10, pp. 1755-1764, Oct. 2000.
[16] T. Pollet, M. Van Bladel, and M. Moeneclaey, "BER sensitivity of OFDM systems to carrier frequency offset and Wiener phase noise," IEEE Trans. Commun., vol. 43, pp. 191-193, Feb./Mar./Apr. 1995.